Electronic Supplementary Material (ESI) for RSC Advances.
This journal is © The Royal Society of Chemistry 2014

Electronic Supplementary Information for

A FRET analysis of dye diffusion in core/shell polymer nanoparticles

Luis Cerdán[1], Eduardo Enciso[2], Leire Gartzia-Rivero[3], Jorge Bañuelos[3], Iñigo López Arbeloa[3], Ángel Costela[1], and Inmaculada García-Moreno[1]*

1 Instituto de Química-Física "Rocasolano" Consejo Superior de Investigaciones Científicas (CSIC), Serrano 119, 28006 Madrid (Spain)

2 Facultad de Ciencias Químicas, Universidad Complutense de Madrid, Ciudad Universitaria, 28040 Madrid (Spain)

3 Facultad de Ciencia y Tecnología, Universidad del País Vasco-EHU, Aptdo. 644, 48080 Bilbao (Spain)

*Corresponding author e-mail: lcerdan@iqfr.csic.es

Estimation of Förster critical radius for the Rh6G/NB system

The FRET rate from an electronically excited donor (D*) to an acceptor (A) separated by a distance r is given by[1,2]

$$w(r) = \frac{1}{\tau_D}\left(\frac{R_0}{r}\right)^6 \tag{S1}$$

where τ_D is the donor lifetime in the absence of acceptors and R_0 is the most characteristic FRET parameter, known as Förster radius and defined as the donor-acceptor separation for which the donor emits and transfers (to the acceptor) its energy with the same probability. R_0 depends on the photophysical properties of donor and acceptor and is given by[3]

$${R_0}^6 = \frac{9000(\ln 10)\kappa^2\phi_f}{128\pi^5 N_A n^4}\int_0^\infty F_D(\lambda)\varepsilon_A(\lambda)\lambda^4 \mathrm{d}\lambda \tag{S2}$$

In Eq. (S2) the integral accounts for the spectral overlap of the normalized donor fluorescence spectrum $F_D(\lambda)$, with the absorption spectrum of the acceptor $\varepsilon_A(\lambda)$ ($M^{-1}cm^{-1}$). ϕ_f and n are the fluorescence quantum yield of the donor in the absence of acceptors and the refractive index of the host medium, respectively, and κ^2 is the orientation factor which accounts for the relative orientation of donor and acceptor transition dipole moments in the host medium.

In the photophysical characterization of the latex nanoparticles, $F_D(\lambda)$, $\varepsilon_A(\lambda)$, and ϕ_f=0.7 have been obtained. Taking into account that the mixture MMA/HEMA/GMA has a refractive index n~1.5 and assuming κ^2~2/3 (isotropic dynamic averaging), one obtains a Förster radius R_0 = 49 Å

Derivation of Eq. 7 in main text: Change in NP size upon growth of multiple shells

The volume occupied in a single NP by the multiple shells (V_S) is given by:

$$V_S = \frac{4\pi}{3}\left(R^3 - R_C^3\right) \tag{S3}$$

where R and R_C are the radii of the NP after and before the shells growth, respectively. Simultaneously, $V_S = m_S/\rho_S$, with m_S and ρ_S being the mass and density of the shells in a single NP. Substituting this expression into Eq. S3 and solving for R one obtains:

$$R = \sqrt[3]{R_C^3 + \frac{3m_S}{4\pi\rho_S}} \tag{S4}$$

On the other hand, the total number of NPs nucleated before the shells growth (N_{NP}) is given by $N_{NP}=M_C/m_C$, where M_C is the total monomer mass introduced in the reactor to nucleate the cores, and m_C is the mass of a single core. If all of the added monomer mass introduced in the reactor to grow the shells (M_S) were used to produced uniform and identical coatings over each NP (no new particles formed, N_{NP} constant), then $m_S=M_S/N_{NP}$ should hold, and hence:

$$m_S = m_C \frac{M_S}{M_C} \tag{S5}$$

Furthermore, $m_C=V_C\cdot\rho_C=4\pi/3R^3{}_C\cdot\rho_C$, with V_C and ρ_C the volume and density of a single core. Substitution of this expression into Eq. S5 leads to:

$$m_S = \frac{4\pi}{3} R_C^3 \frac{M_S}{M_C} \rho_C \tag{S6}$$

Finally, introducing Eq. S6 into Eq. S4, reordering terms, and introducing the ratio $r=M_S/M_C$, one arrives to Eq. 7 in the main text.

$$\left(\frac{R}{R_C}\right)^3 = \left(\frac{d}{d_C}\right)^3 = 1 + r\frac{\rho_C}{\rho_S}$$

The previous derivation assumes several issues, including that the NPs are monodispersed, all of the shells have the same density, and the polymerization yield of core nucleation and shell growth is the same. Hence, Eq. (7) must be considered as the ideal case.

Fit expressions for FRET analysis in spherical NPs

Model 1: Core/Surface distributions:

The dye distribution in a Core/Surface NP can be described mathematically as $C_{D,A}(R) = C^S_{D,A}\delta(r_D-R_S) - (C^S_{D,A}-C^C_{D,A})H(R_S-r_D)$, where $C^S_{D,A}$ and $C^C_{D,A}$ are the surface and volume densities of donors and acceptors in the surface (S) and the core (C), respectively, $H(R_S-r_D)$ and $\delta(r_D-R_S)$ are the Heaviside step function and the

Dirac delta function, respectively, and R_S is the nanoparticle radius. Substitution of this expression into Eq. 4 of the main text yields:

$$I_D(t) = 4\pi C_D^S R_S^2 \exp\left\{-\frac{t}{\tau_{D,S}}\right\}\exp\{-(g_1(t)+g_2(t))\} + 4\pi C_D^C \exp\left\{-\frac{t}{\tau_{D,C}}\right\}\int_0^{R_S} r_D^2 \exp\{-(g_3(r_D,t)+g_4(r_D,t))\}dr_D \quad \text{(S7)}$$

$$\begin{aligned}
g_1(t) &= 2.12705 C_A^S R_0^2 2\left(\frac{t}{\tau_{D,S}}\right)^{1/3} \times \left(1 + 0.0231\left(\frac{R_0}{R_S}\right)^4\left(\frac{t}{\tau_{D,S}}\right)^{2/3} - 7.21\times10^{-5}\left(\frac{R_0}{R_S}\right)^{10}\left(\frac{t}{\tau_{D,S}}\right)^{5/3}\right)\\
g_2(t) &= 3.71222 C_A^C R_0^3 2\left(\frac{t}{\tau_{D,S}}\right)^{1/2} \times \left(1 + 0.566785\left(\frac{R_0}{R_S}\right)\left(\frac{t}{\tau_{D,S}}\right)^{1/6} - 0.035262\left(\frac{R_0}{R_S}\right)^3\left(\frac{t}{\tau_{D,S}}\right)^{1/2}\right)\\
g_3(r_D,t) &= \frac{2\pi C_A^S R_S}{r_D}\int_{(R_S-r_D)}^{(R_S+r_D)} \mathrm{d}r\, r\left[1-\exp\left\{-\frac{t}{\tau_{D,C}}\left(\frac{R_0}{r}\right)^6\right\}\right]\\
g_4(r_D,t) &= 4\pi C_A^C \int_{\min\{R_S-r_D,r_{\min}\}}^{R_S-r_D} \mathrm{d}r\, r^2\left[1-\exp\left\{-\frac{t}{\tau_{D,C}}\left(\frac{R_0}{r}\right)^6\right\}\right] +\\
&\quad + \frac{\pi C_A^C}{r_D}\int_{\max\{R_S-r_D,r_{\min}\}}^{(R_S+r_D)} \mathrm{d}r\, r\left(R_S^2-(R-r)^2\right)\left[1-\exp\left\{-\frac{t}{\tau_{D,C}}\left(\frac{R_0}{r}\right)^6\right\}\right]
\end{aligned} \quad \text{(S8)}$$

where $\max\{a,b\}$=1/2(a+b+|a-b|) and $\min\{a,b\}$=1/2(a+b-|a-b|), and

$$r_{\min} = \frac{0.554}{\sqrt[3]{C_A^C}} \quad \text{(S9)}$$

We allow the donor to have different lifetimes in the core ($\tau_{D,C}$) and the surface ($\tau_{D,S}$). The fitting parameters are C^C_A, C^S_A, C^C_D, and C^S_D. Nevertheless, as the donor and acceptor molecules have very similar nature (both chemical and electrostatic), they will have similar affinities for a given monomer mixture, hence, we assume that both dyes will present the same dye distribution, i. e., $C^C_A/C^S_A = C^C_D/C^S_D$. This constraint reduces the degrees of freedom to C^C_A and C^S_A.

Model 2: Core/Shell distributions:

The dye distribution in a generic Core/Shell nanoparticle is given by $C_{D,A}(R) = C^S_{D,A}H(R_S-r_D) - (C^S_{D,A}-C^C_{D,A})H(R_{SC}-r_D)$, where $C^S_{D,A}$ and $C^C_{D,A}$ are the volume density of donor and acceptor in the shell (S) and the core (C), respectively, and R_{SC} is the core radius. Substitution of this expression into Eq. 4 of the main text results in:

$$\begin{aligned}
I_D(t) &= 4\pi C_D^S \exp\left\{-\frac{t}{\tau_D}\right\}\int_0^{R_S} r_D^2 \exp\{-g_1(r_D,t)+g_2(r_D,t)\}dr_D\\
&\quad - 4\pi(C_D^S - C_D^C)\exp\left\{-\frac{t}{\tau_D}\right\}\int_0^{R_{SC}} r_D^2 \exp\{-g_1(r_D,t)+g_2(r_D,t)\}dr_D
\end{aligned} \quad \text{(S10)}$$

$$
\begin{aligned}
g_1(r_D,t) &= 4\pi C_A^S \int_{\min\{R_S-r_D,\,r_{\min}^S\}}^{R_S-r_D} \mathrm{d}r\, r^2 \left[1-\exp\left\{-\frac{t}{\tau_D}\left(\frac{R_0}{r}\right)^6\right\}\right] + \\
&+ \frac{\pi C_A^S}{r_D} \int_{\max\{R_S-r_D,\,r_{\min}^S\}}^{(R_S+r_D)} \mathrm{d}r\, r\left(R_S^2-(R-r)^2\right)\left[1-\exp\left\{-\frac{t}{\tau_D}\left(\frac{R_0}{r}\right)^6\right\}\right] \\
g_2(r_D,t) &= 4\pi\left(C_A^S-C_A^C\right) \int_{\min\{R_{SC}-r_D,\,r_{\min}^C\}}^{R_{SC}-r_D} \mathrm{d}r\, r^2 \left[1-\exp\left\{-\frac{t}{\tau_D}\left(\frac{R_0}{r}\right)^6\right\}\right] \\
&+ \frac{\pi\left(C_A^S-C_A^C\right)}{r_D} \int_{\max\{R_{SC}-r_D,\,r_{\min}^C\}}^{(R_{SC}+r_D)} \mathrm{d}r\, r\left(R_{SC}^2-(R-r)^2\right)\left[1-\exp\left\{-\frac{t}{\tau_D}\left(\frac{R_0}{r}\right)^6\right\}\right]
\end{aligned}
\tag{S11}
$$

where we have assumed that the lifetime of the donor in core and shell are the same. The fitting parameters are C^C_A, C^S_A, C^C_D, and C^S_D. Again we can assume $C^C_A/C^S_A = C^C_D/C^S_D$. In addition:

$$
r_{\min}^{C,S} = \frac{0.554}{\sqrt[3]{C_A^{C,S}}} \tag{S12}
$$

Theoretical evaluation of dye diffusion in core/shell NPs

With the aim to have a clearer understanding of the diffusion processes within core/shell NPs (equilibrium and transient dye distributions, time scales, *etcetera*), we decided to analyze the behavior predicted by existing diffusion models. In this sense, Fick's second law[4] predicts how diffusion causes the concentration of a given element to change in space and time for a given diffusion coefficient (dependent on the particular material properties). Fick's second law reads:

$$
\frac{\partial C}{\partial t} = \nabla\cdot\left(D\nabla C\right) = D\nabla^2 C + \nabla D\cdot\nabla C \tag{S13}
$$

where C is the volume number concentration (nm^{-3}) of the diffusive element and D is the diffusion coefficient along the NP radius in units of cm^2s^{-1}. As we are dealing with spherical NPs, we use spherical coordinates, and since the dye distributions present spherical symmetry ($C=C(r;t)$ and $D=D(r)$), the axial and azimuthal derivatives vanish, so that:

$$
\begin{aligned}
\nabla D\cdot\nabla C &= \frac{\partial D}{\partial r}\frac{\partial C}{\partial r} \\
\nabla^2 C &= \frac{1}{r^2}\frac{\partial}{\partial r}\left(r^2\frac{\partial C}{\partial r}\right) = \frac{2}{r}\frac{\partial C}{\partial r} + \frac{\partial^2 C}{\partial r^2}
\end{aligned}
\tag{S14}
$$

Substituting Eqs. S14 into Eq. S13, Fick's second law simplifies to:

$$
\frac{\partial C}{\partial t} = D\frac{\partial^2 C}{\partial r^2} + \frac{2D}{r}\frac{\partial C}{\partial r} + \frac{\partial D}{\partial r}\frac{\partial C}{\partial r} \tag{S15}
$$

As the NPs we are dealing with present core/shell morphologies with different, but homogeneous, monomer mixtures in core and shell, we may assume that each region will present different, but constant, diffusion

coefficients D_C and D_S for core and shell, respectively. In other words, the diffusion coefficient along the NP can be mathematically described as $D(r)= D_S H(R_S-r)-(D_S-D_C)H(R_{SC}-r)$, where $H(R_S-r)$ is the Heaviside step function, R_S is the NP external radius, and R_{SC} is the core radius.

Since we are dealing with a chemical system in which every region, due to its different composition, presents a different affinity for the dyes, it is more adequate to work with chemical potentials. The chemical potential inside the NPs is:

$$\mu(r,t) = \mu^0(r) + RT \ln a(r,t) \tag{S16}$$

where $a(r,t)$ is the dye activity in the polymer matrix, $\mu^0(r)$ is the reference chemical potential of a solution with an activity equal one ($\mu^0(r)=\mu_C{}^0$ for $0<r<R_{SC}$ and $\mu^0(r) = \mu_S{}^0$ for R_{SC} <r<R_S), R=8.31 $JK^{-1}mol^{-1}$ is the gas constant and T=300 K is the matrix temperature. Particle regions with large affinity for the dye (high solubility) will reduce the reference chemical potential and will enhance the dye concentration. At low concentrations, as the ones in our NPs, the activity can be replaced by the local dye concentration, *i. e.*, $a(r,t)\approx C(r,t)$. Then, concentration and chemical potential are related as:

$$C(r,t) = \exp\left(\frac{\mu(r,t) - \mu^0(r)}{RT}\right) \tag{S17}$$

Substitution of Eq. S17 into Eq. S15 yields:

$$\frac{\partial \mu}{\partial t} = D\left(\frac{\partial^2 \mu}{\partial r^2} + \frac{1}{RT}\left(\frac{\partial \mu}{\partial r}\right)^2\right) + \frac{2D}{r}\frac{\partial \mu}{\partial r} + \frac{\partial D}{\partial r}\frac{\partial \mu}{\partial r} \tag{S18}$$

Eq. S18 is not defined at $r= R_{SC}$, as the term $\partial D/\partial r \cdot \partial \mu/\partial r$ diverges due to the mathematical description used for the core/shell properties. Experimentally this term does not diverge, as there is a smooth transition in both D and μ (or C) from core to shell. Hence, we can assume heuristically that the values of D and μ at R_{SC} are the mean of the values of D and μ at either side of the interphase, *i. e.*:

$$\begin{aligned} D(R_{SC}) &= \frac{(D(R_{SC}+\delta r) + D(R_{SC}-\delta r))}{2} \\ \mu(R_{SC},t) &= \frac{(\mu(R_{SC}+\delta r,t) + \mu(R_{SC}-\delta r,t))}{2} \end{aligned} \tag{S19}$$

where δr is half the thickness of the interphase and will be, in practice, the numerical spatial integration step. As we assume that no dyes can enter or leave the NP (*i. e.*, the system is perfectly insulated), the von Neumann boundary condition applies to this system of equations, so that:

$$\left.\frac{\partial \mu}{\partial r}\right|_{r=R_S} = 0 \tag{S20}$$

As initial conditions we use those of sample CS1:

$$\begin{aligned}
&\mu_A(R_{SC} < r \le R_S, t = 0) = \mu_S^0 + RT\ln C_{A0} \\
&\mu_A(0 \le r < R_{SC}, t = 0) \to -\infty \\
&\mu_D(R_{SC} < r \le R_S, t = 0) \to -\infty \\
&\mu_D(0 \le r < R_{SC}, t = 0) = \mu_C^0 + RT\ln C_{D0}
\end{aligned} \tag{S21}$$

These initial conditions have to be taken with care, since they are idealistic, as they assume that the dye diffusion process begins once the shell is completely formed. Experimentally, the shell needs some time to grow, and during this growing process, the dye diffusion would take place. Nevertheless, the final equilibrium state computed with the above system of equations will be more realistic, since is independent on the initial state.

Then, to obtain the time evolution of the dye concentration profile in the NPs, being what can be evaluated by means of FRET, Eq. S18 is numerically solved with boundary and initial conditions of Eqs. S19-S21, and the computed chemical potential is substituted at each time step into Eq. S17. To solve this problem the values of μ_C^0, μ_S^0, D_C and D_S are needed, but they are not well defined for these nanostructured material and, consequently, they have to be estimated attending to some particular properties of the NPs. All systems evolve to the equilibrium by compensating the differences in the chemical potentials along the system, *i. e.*, at equilibrium $\mu(r)$=constant $\forall r$. For our particular case, this equilibrium condition implies that $\Delta\mu^0=\mu_C{}^0-\mu_S{}^0=RT\ln(H)$, where $H=C_{eq}{}^S/C_{eq}{}^C$ is the partition ratio and $C_{eq}{}^S$ and $C_{eq}{}^C$ are the equilibrium concentrations in the shell and core, respectively. Hence, by making use of the $C_A{}^S$ and $C_A{}^C$ values obtained from the fit to the fluorescence intensity decay of sample CS1 (Fig. 2a), it can be heuristically inferred that, in the particular case of this sample, $\Delta\mu^0\approx RT\ln(2)$.

On the other hand, the absolute values for D_C and D_S are not very relevant for our purposes, as we look for a qualitative understanding of the problem. In fact, the absolute value of D has no influence on the equilibrium distribution, but it affects the time scales (the higher D is, the quicker the equilibrium is reached). Nevertheless, we chose diffusion coefficients in the order of 10^{-16} cm^2s^{-1}, much lower than the ones for large dyes diffusing in PMMA below glass transition temperature[5] in which diffusion is highly hindered. Indeed, in our case the diffusion coefficient would be much higher, since the NP could be partially swallowed with water, the dye molecules are reduced in size, and during the synthesis the temperature is raised, facts that favors dye diffusion. Hence, the time scales evaluated in the following could be taken as upper limits of the actual situation. As for the particular ratio D_C/D_S, we may assume that it is slightly higher than 1, meaning that that the dyes move much more freely in the core than in the shell, which is consistent with the different monomer compositions used for both regions (Table 1). For the core we used MMA, HEMA and GMA, monomers which hardly cross-link upon polymerization, and so the core will be composed by a linear copolymer. On the other hand, for the shell we used MMA, HEMA, GMA and the cross-linker monomer EGDMA, which results in the shell being a cross-linked copolymer. Cross-linked polymers are known to have smaller free volumes than linear polymers,[6] while it is known that the higher the free volume is, the higher the diffusion coefficient becomes.[7] Consequently, the core, which is made of a linear copolymer with higher free volume, would present a higher diffusion coefficient. Nevertheless, as explained before, the particular choice of D_C/D_S has a limited effect on the present problem, and will be considered as unity for simplicity.

Computed chemical potential along the NP radius as a function of time for sample CS1

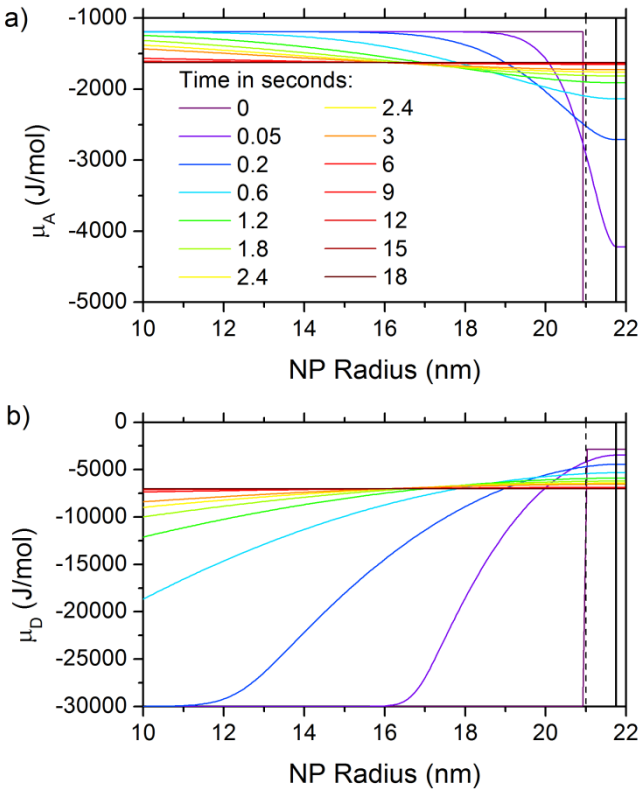

Figure S1 Chemical potential along a NP analogous to CS1 as a function of time both for a) the acceptor and b) the donor. For better inspection, only the region from 10 nm is shown. The solid and dashed vertical lines indicate the position of the NP and core radii, respectively.

References:

(1) Förster, T. *Ann. Phys.* 1948, **2**, 55-75.
(2) Förster, T. *Z. Naturforsch.* 1949, **4A**, 321-327.
(3) Farinha, J. P. S., Martinho, J. M. G. *J. Phys. Chem. C* 2008, **112**, 10591-10601.
(4) Cussler, E. L. *Diffusion*, 1st Ed., Cambridge University Press, Cambridge, 1984.
(5) Stempfle, B.; Dill, M.; Winterhalder, M. J.; Müllen, K.; Wöll, D. *Polym. Chem.* 2012, **3**, 2456-2463.
(6) Dlubek, G.; Stejny, J.; Alam, M. A. *Macromolecules* 1998, **31**, 4574-4580.
(7) Duda, J. L. *Pure & Appl. Chem.* 1985, **57**, 1681-1690.